Numerical modelling of shear behaviour of reinforced concrete pile caps

by

Alan G. Bloodworth[1], Jing Cao[2] and Ming Xu[3]

Abstract

The application of bending theory based methods and strut-and-tie models for the design of pile caps to resist shear is still a subject of debate, with the latest Eurocodes permitting both methods but not giving much guidance as to their use. The former UK design standards for concrete buildings and bridges, recently withdrawn, gave more guidance and it is likely that these methods will continue to be used by designers. However, there is considerable discrepancy between these standards, particularly with regards to the width of cap over which shear enhancement at short spans may be applied, and how much longitudinal reinforcement to take as a tie in the strut-and-tie method. Both standards are also seen as conservative.

To gain a better understanding of the problem and assess the available design methods, nonlinear finite element analysis has been performed to investigate the shear behaviour of four-pile reinforced concrete pile caps, under full-width wall loading. The models were validated against an experimental programme that included an optical photogrammetric method for measuring full-field displacements. An extensive parametric study was carried out, varying shear span, cap width and reinforcement ratio over a practical range.

The conservatism of the UK design standards, and the real shear capacity of the pile caps, were found to be a function of shear enhancement factor and the width of the

cap over which shear enhancement is applied. Strut-and-tie behaviour was observed in the models, and a commonly used strut-and-tie method was found to give fairly good predictions. A modified strut-and-tie method is suggested for this particular configuration of a four-pile cap under full-width loading, which gives more accurate predictions. This is especially so for samples with large transverse pile spacing where a significant proportion of the longitudinal reinforcement over the width of the cap can be assumed to participate in the yielding ties.

CE Database subject headings: Pile caps; Shear resistance; Reinforced concrete; Finite element analysis

1.   Lecturer, School of Civil Engineering and the Environment, University of Southampton, SO17 1BJ, UK. Email: A.G.Bloodworth@soton.ac.uk

2.   Structural engineer, BG&E Pty Limited, 484 Murray Street, Perth, WA 6000, Australia. Email: jing.cao@bgeeng.com

3.   Lecturer, Department of Civil Engineering, Tsinghua University, Beijing 100084, China. Email: mingxu@mail.tsinghua.edu.cn

Numerical modelling of shear behaviour of reinforced concrete pile caps

by

 A. G. Bloodworth, J. Cao and M. Xu

Introduction

A reinforced concrete (RC) pile cap is an example of a short-span, relatively deep beam which can also be wide relative to its depth if the transverse pile spacing is large, such that two-dimensional spanning behaviour can become significant. The design standards contain two main methods for their design to resist shear. The first is deep beam theory, developed by Regan (1971) for one-way spanning beams, in which the assumption is made of a critical opening inclined shear crack, above which is a compression zone of concrete. Shear failure occurs when the concrete fails in compression. The depth of the concrete compression zone is related to the relative rotation of the two surfaces of the crack.

The second is the strut-and-tie method (STM) which is based on the concept of longitudinal and transverse bottom reinforcement acting as ties with inclined compressive struts joining the pile heads and the centre of application of the load (Adebar and Zhou 1996).

There is discrepancy between the deep beam theory based design formulae in the UK design standards BS 8110 (BSI 1997) and BS 5400 (BSI 1990) due to different definitions of the width of the cap for which shear enhancement may be applied, that lead to differences of a factor of two or three between predicted capacities. This

discrepancy has not been resolved in the Eurocodes (BSI, 2004; BSI, 2005). US and Canadian standards (AASHTO 2007; ACI 2005; CSA 1994) favour STM, but there has been uncertainty expressed about its applicability (Park et al 2008). Fundamentally overall only a limited experimental data set is available to verify the current design approaches (Bloodworth et al. 2003).

Tests of the shear capacity of a series of reduced-scale pile caps under full-width wall loading (Fig. 1) with uniform bottom reinforcement in both directions have been carried out (Cao and Bloodworth 2011). It was found that both UK code deep beam theory based design formulae gave conservative predictions. The strut-and-tie method in the standards gave better predictions, suggesting the shear behaviour of a pile cap can be described physically in this way, but becomes conservative when transverse pile spacing is large.

This paper describes the development of nonlinear finite element analysis (FEA) models of the experimental samples and their verification against the experimental results. The FEA has then been extended to cover a wider range of pile cap dimensions by means of a parametric study of 88 further analyses. Two-way behaviour of the caps under load was observed in the FEA, and it became apparent that the STM indeed provides a reasonable physical description of the shear behaviour. The results from the parametric study are used to suggest a modified STM which gives improved predictions of capacity, especially for wide transverse pile spacing.

Design rules for shear enhancement in pile caps

UK standards BS 8110 and BS 5400 apply to pile caps design formulae originally developed for one-way spanning RC beams. The formulae express the design concrete shear stress v_c in terms of the beam width b, effective depth d, concrete characteristic cube strength f_{cu} and longitudinal main reinforcement area A_s. Because pile caps are relatively short span deep structures, enhancement of shear strength by the factor $2d/a_v$ is usually applicable, where a_v is the shear span. BS 8110 and BS 5400 have different rules for the width of the cap over which shear enhancement may be considered effective. BS 8110 allows it to be the sum of the widths of zones centred on each pile head, where each zone may be up to three times the pile diameter in width. In BS 5400 the corresponding zones are limited to only one pile diameter in width over each pile head.

The Eurocode for concrete design (BSI 2004) has less specific guidance for pile caps (Clause 9.8.1) than the UK Standards. It stipulates similar deep beam theory based formulae, but with a different depth factor. However, specific guidance on the width of the cap for which shear enhancement is effective is lacking. The main clauses for shear design state that shear enhancement can only be applied provided 'the longitudinal reinforcement is fully anchored at the support' (Clause 6.2.2). If the 'support' is taken as meaning strictly only the piles, then this is the same as the BS 5400 provision. However, a possible interpretation of the Eurocode is that the piles in the transverse direction may provide a type of 'line of support', in which case designers may opt for the BS 8110 approach or even take the enhancement as effective across the entire cap width.

Pile cap experiments

A total of 17 reduced-scale pile cap samples in four batches were tested (Cao 2009). Figure 2 shows the experimental setup used to achieve the configuration of loading and supports shown in Figure 1. Results from the most successful final batch of nine samples are reported in Cao and Bloodworth (2011) and are used for the verification of the FEA described herein.

The depth h in Figure 1 was kept constant at 230 mm, the pile diameter h_p at 130 mm, the width h_c of the loading spreader beam at 100 mm and the pile depth d_p at 260 mm. The remainder of the dimensions that were varied are given in Table 1 for the nine samples, along with the reinforcement details and concrete strengths for each cap. The parameter μ is the ratio between transverse pile spacing and pile diameter ($\mu = {l_y}/{h_p}$).

Reinforcement was uniformly distributed with equal percentages in both directions. Mean reinforcement yield strength f_y of 547 N/mm^2 and mean ultimate strength of 646 N/mm^2 were obtained by testing. Concrete cube strength f_{cu} was the mean of three results for each pile cap, on 100 mm cubes. Cylinder strengths are calculated in Table 1 from the cube strengths using the relationship in Table 3.1 of the Eurocode (BSI 2004).

The 150-tonne Instron column-testing machine at the University of Southampton was used. The hydraulic actuator lifts the lower steel platen. Soft boards were placed between the top platen, spreader beam and cap to avoid stress concentrations causing local crushing. The pile cap was set on the lower platen temporarily supported on wedges and self-levelling screed poured underneath the piles to ensure an even contact area. Horizontal restraint at the pile bases was minimised by means of plastic

sheets under the piles between which oil was placed. The pile bases experienced a combination of vertical and moment reactions, but because the pile bending stiffness was much lower than the cap, analysis showed that the hogging moment applied to the cap at the top of the piles was small.

The caps were instrumented to measure load, and displacements recorded by linear potentiometers distributed over the soffit. Crack distribution and propagation were highlighted by hand on the surfaces and photographed. In addition, a full-field distribution of strain on the front surface of the cap was obtained using digital photogrammetry (Cao et al 2007). Results from the experiments, including the development of cracking with load, final crack patterns and typical load-displacement date are given in Cao and Bloodworth (2011).

The 'shear enhancement application factor', A, is defined as:

$$A = b_{enh}/b \qquad\qquad (1)$$

Where b_{enh} is the width over which shear enhancement is considered effective according to BS 8110 (*i.e.* sum of width of all relevant strips centred on pile heads), and b is the overall cap width. The experimental samples consisted of two series. In Series A, a_v/d was varied with A constant, by varying longitudinal pile spacing with constant transverse pile spacing. Series B was designed *vice versa* to vary A under constant a_v/d, by varying the transverse pile spacing with constant longitudinal pile spacing. It had a lower reinforcement ratio than Series A so the effect of this quantity could also be investigated.

Numerical model

The software used was the commercial FEA package DIANA, which has been shown to give satisfactory results in the analysis of continuous RC beams without shear reinforcement (Keown 2000).

Taking advantage of symmetry, only one quarter of the cap was modelled (Fig. 3), with displacements constrained perpendicular to the cut surfaces. Nodes on the pile base were supported vertically but released in the two horizontal directions, to mimic the experimental setup (Cao and Bloodworth 2011). A downwards prescribed displacement was applied over the area of the full-width wall loading.

20-node isoparametric solid brick elements with a quadratic interpolation function and $3 \times 3 \times 3$ gauss integration scheme (DIANA 2002) were used. Ten mesh layers were used in the cap body, with increased mesh density in the region under the wall loading.

Reinforcement was modelled as a thin sheet at the level of the axis of the reinforcing bars in the experimental samples. Perfect bond between reinforcement and concrete was assumed. Piles were modelled as unreinforced, as it was proved that negligible contribution was given by the pile reinforcement to pile bending and compression stiffness (Cao 2009).

Concrete is assumed to behave linearly before yield in both compression and tension, with Young's modulus of 28 GPa and Poisson's ratio of 0.2. f_{cu} was obtained from cube tests, and concrete tensile strength f_t taken as $f_{cu}/10$. In the nonlinear stage for concrete in tension, a smeared cracking model with fixed angle of cracks and constant tension cut-off was used. Linear tension softening was assumed after peak tensile

strength is reached (Fig. 4), with ultimate crack strain ε_{ult}^{cr} taken as 0.000311 (DIANA 2005).

For concrete in compression, the von Mises failure criterion was used, with ideal plasticity without hardening or softening and infinite maximum compressive strain. The yield stress was taken as f_{cu} and shear retention factor as 0.2. For reinforcement, Young's modulus was taken as 210 GPa, and in the non-linear stage, the von Mises failure criterion was used for both compression and tension, assuming again ideal plasticity and infinite maximum strain. Yield stress f_y was taken as 547 MPa.

A Newton-Raphson solver was used, with convergence criterion on the energy norm ratio between two consecutive iterative steps (DIANA 2002). Prescribed displacement step in the range 0.05 mm – 0.4 mm were applied.

Model validation

Validation was performed against load-deflection curves and crack distributions. A primary parameter was ultimate crack strain ε_{ult}^{cr}, for which the recommended control value is 0.000311 (DIANA 2005). ε_{ult}^{cr} can also be obtained from the energy absorbed during maturing of a crack by calculating G_f, the fracture energy consumed in the formation and opening of all micro-cracks per unit area of plane ahead of the tip of the advancing crack (Bazant et al. 1983). Calculated this way, ε_{ult}^{cr} was around 0.003 for both reinforced concrete ($\varepsilon^{cr} = f_y / E_s$) and unreinforced concrete ($\varepsilon^{cr} = \dfrac{2G_f}{f_t h_{cr}}$, where h_{cr} is the crack band width) (Cao 2009). Figure 5 shows load-displacement

curves for ε_{ult}^{cr} from $0.000311 - 0.006$ for cap B4A1. The larger ε_{ult}^{cr}, the stiffer the structure response. However, the actual failure load does not vary with ε_{ult}^{cr}, so the control value of 0.000311 was adopted for all the analyses.

Figure 6 shows an observed crack pattern on a cap front surface at the failure step compared with that predicted from FEA. Both show large inclined shear cracks, hogging cracks above the pile head and considerable central bending cracks.

Table 2 compares FEA failure loads with experiments. The ratio of FEA to experimental failure load is close to 1.0 for B4A4, B4A5 and B4B4. Some of the remaining caps did not fail completely across their whole width in the experiments due to asymmetric loading (Cao and Bloodworth 2011), so their true failure load should have been higher, hence explaining their ratio being above 1.0 (particularly B4A2).

It was concluded from the validation that the FEA gave an adequate representation of the experimental results (particularly failure load) with the parameters chosen, making them suitable for use in the extended parametric study described later.

Model output

In the experiments, a full-field strain distribution on the cap front surface was obtained by digital photogrammetry (Cao et al. 2007). Concrete strain at the level of the main longitudinal reinforcement was observed in all cases to be greater than the reinforcement yield strain of 0.0026 over the whole longitudinal span. Thus it is likely the reinforcement was acting as a yielding tie at ultimate load. This observation is

supported by the FEA of most samples. For example, for B4B2 (Fig. 7) σ_{sx} reaches yield (547 MPa) over almost the whole longitudinal span, for the width of the pile head and between the pile and the front surface. Between the piles, σ_{sx} reaches yield at mid longitudinal span but reduces significantly towards the line of pile support, suggesting two-way spanning behaviour.

This two-way behaviour is confirmed by the stress in the transverse reinforcement σ_{sy}. Transverse ties under significant elastic stress are observed concentrated over the pile head, with stress greater for larger transverse pile spacing. For example in B4A5 ($\mu = 2.3$), σ_{sy} peaks at 80 MPa, whereas for B4B3 ($\mu = 4.23$) (Fig. 8) σ_{sy} peaks at 240 MPa. This implies potential for bending or shear cracking in the transverse direction.

In all the FEA of the experimental samples, diagonal splitting cracks linking the wall loading to the pile head are present at the onset of yield and mature at the failure step *e.g.* B4A1 (Fig. 6).

The observations of a yielding main longitudinal reinforcement tie, a transverse tie at elastic stress which depends on transverse pile spacing and diagonal compressive splitting cracks point towards strut-and-tie behaviour.

Von Mises stress σ_v and crack strain ε^{cr} can be observed in the FEA output. Figure 9(a) shows a zone in compression between the pile head and the loaded area, idealised as an equivalent strut linking the pile head with a point under the wall loading

between the centre of the cap top and the top front edge. Figure 9(b) shows the distribution of ε^{cr}, highlighting diagonal cracking at the onset of failure.

Parametric study

The FEA was extended with 88 further models under full-width wall loading, with the range of key dimensions shown in Figure 10. Other dimensions indicated in Fig. 1 were consistent with the experimental samples. The range of a_v/d and μ for the experimental samples is indicated by the bold dash lines.

The geometry idealisation, boundary conditions, element type and constitutive models for concrete and reinforcement were as previously. The reinforcement in the cap was 12 mm bars at 50 mm spacing in both directions, and the piles were again unreinforced but with an artificially high strength. Concrete Young's modulus was taken as 28 GPa, Poisson's ratio as 0.2, f_{cu} as 25 MPa and f_t as 2.5 MPa. Ultimate crack strain ε_{ult}^{cr} was taken as 0.001 to improve convergence.

The Newton-Raphson solver was again used, with the threshold energy norm ratio varied over a range 0.005 to 0.05, wider than the range 0.01 to 0.02 used previously to cater for some brittle failures that occurred. Prescribed displacement step size was from 0.2 mm to 2 mm.

Predicted failure loads

Figure 11 plots the failure load of the cap V as a function of longitudinal and transverse pile spacings l_x and l_y. V increases as expected with increasing l_y and μ and decreasing l_x (decreasing a_v/d).

Figure 12 shows the relationship between average shear stress at failure v, a_v/d and A (μ). At large μ, the cap becomes more two-way spanning and v becomes less dependent on a_v/d, especially for $a_v/d < 0.81$; the proportion of cap width over which shear enhancement is effective is decreasing. For smaller a_v/d, *e.g.* < 0.31, this trend continues with v reducing noticeably once μ increases beyond 3.0.

Predicted failure mechanisms

Most parametric study models had ductile failures that were either in bending or shear judged by the crack distribution on the front surface, and in the latter case by the occurrence of a yielding reinforcement tie over the whole longitudinal span (Figure 10). Caps with large l_x failed by bending with wide midspan cracks (*e.g.* Fig. 13) and stress in the longitudinal reinforcement σ_{sx} increasing towards midspan (Fig. 14). Diagonal splitting cracks on the front surface become more apparent at smaller a_v/d, as for B4A4 (Fig. 9).

For the majority of caps, the longitudinal reinforcement yielded across the whole width of the cap at midspan, either in shear or bending failure. Figure 15 shows the range with large l_y ($\mu > 4$) and relatively small l_x for which this was not the case and in which yielding occurs on a strip over each pile head (*e.g.* Fig. 16). With larger l_x, the yielding strip can be wider than three times pile diameter when $\mu > 3$, even extending across the whole cap width (Fig. 17).

In the transverse direction, significant reinforcement stress σ_{sy} >200 N/mm^2 occurred in caps with μ >= 2. As μ increases, σ_{sy} increases and can reach yield (Fig. 18). Normally the transverse tie concentrates on the pile head.

Comparison with current design formulae

In the following discussion, the ratio of failure load predicted by FEA to those from deep beam theory based shear formula and STM in BS 8110 is denoted $\beta_{BS8110b}$ and $\beta_{BS8110S}$ respectively. In each case, the partial factor on material strength γ_m = 1.0.

The variation of $\beta_{BS8110b}$ against a_v/d and A (μ) proved to be in the range 2.03 to 3.10 (Cao 2009), showing consistent conservatism in BS 8110. A global multiplying factor of 2.0 could be applied to the BS 8110 formula, although this would lack clear physical meaning.

A strut-and-tie model is permitted as an alternative design method in the British Standards, with the model comprising concrete struts transferring the load from the centre of the loaded area to the centres of each pile head, reacted by reinforcement ties in both directions (Bloodworth et al 2003; Clarke 1973). The standards differ in the amount of longitudinal reinforcement assumed or permitted to participate in the longitudinal tie. BS 8110 envisages the longitudinal reinforcement as uniformly distributed across the cap width, with the longitudinal ties to be the reinforcement within strips no wider than three times the pile diameter centred on the piles. In BS 5400, all longitudinal reinforcement can included in the ties, provided 80% of it is

placed in strips anchored directly over the pile heads. The BS 8110 approach is seen as more practical, as concentrating the reinforcement over the pile heads in line with BS 5400 can cause problems with punching shear, especially under concentrated loads. Neither standard considers the strength of the concrete strut, although this is addressed in the Eurocodes (BSI 2004) and in US and Canadian standards.

Eurocode detailing provisions state that the longitudinal reinforcement should be concentrated in the 'stress zones between the tops of the piles' (BSI 2004; BSI 2005). This may be taken by designers to mean entirely confined to over the pile heads, in which case the implication is that all such reinforcement may be taken to participate in the longitudinal tie. US Standards have a similar provision that longitudinal reinforcement should be anchored in the nodal zones in the strut-and-tie model.

Figure 19 shows the variation of $\beta_{BS8110S}$ with a_v/d and A (μ). At small pile transverse spacing ($A = 1$), the STM matches well with FEA, whilst for large transverse pile spacing ($A < 1$ or $\mu > 3$) the FEA failure load is higher than from the STM. This can be explained by the longitudinal yielding tie being wider than the limit of three times the pile diameter in BS 8110 and even extending over the whole cap width when $\mu > 3$ (*e.g.* Fig. 17). A yielding tie can also form in the transverse direction (Fig. 18).

Improved strut-and-tie method

The experiments and FEA have shown that the longitudinal tie is usually wider than the pile diameter, and at large transverse pile spacing it can exceed three times the pile diameter. Additionally there can be significant stress in the transverse reinforcement. A new STM formulation is thus proposed, based on the strut and tie arrangement

shown in Figure 20. 90% of the longitudinal reinforcement area A_s (assumed to be uniformly distributed) is included in the ties, regardless of the transverse pile spacing to diameter ratio. In addition, the top of the inclined concrete strut is relocated slightly to link a point one quarter of the width of the loaded area h_c from the transverse centreline of the cap (and $(1/4)h_c.\tan \alpha$ from the longitudinal centreline of the cap) to the centre of the pile head, for all load patterns, thus accounting for the width of the wall loading and pile. The total load capacity predicted by this new STM is:

$$F = \frac{4zf_y(0.9A_s)}{l_x - h_c/2} \qquad (2)$$

Where z is the inner lever arm. The ratio β_{nSTM} of the shear capacity predicted by FEA to that from the new STM is shown in Figure 21, where z has been taken as $0.9d$. Compared with $\beta_{BS8110S}$ (Fig. 17), β_{nSTM} is closer to 1.0 over a larger range of cap sizes. The prediction is particularly good over the range of a_v/d and μ covered by the experimental samples representing a practical range of pile cap dimensions, indicated by the bold lines.

The triangular region in the corner of the curve plane in Figure 21 where β_{nSTM} drops below 1.0, indicated by the dashed line has vertices $\mu = 4.0$, $a_v/d = 0.31$ and $\mu = 9.2$, $a_v/d = 1.0$ approximately. In this region, it is becoming a poor assumption for the longitudinal tie to be as wide as 90% of the cap width, *e.g.* as seen in Figure 16 ($\mu = 9.2$, $a_v/d = 0.31$). However, this region represents caps which have both large transverse pile spacing (relative to pile diameter) and large shear enhancement factor (*i.e.* short longitudinal pile spacing relative to cap effective depth). This geometry is not a very practical range, and indeed under the Eurocodes, a_v/d is limited to be no less than 0.5 in the calculation of shear enhancement.

Conclusions

Non-linear FEA has been carried out to investigate shear capacity and behaviour of pile caps under full-width wall loading, verified against the results of a series of reduced-scale experiments. The most important observation from the FEA, backed by the experimental observations, is that a strut-and-tie model is a valid representation of the shear behaviour of deep two-way pile caps.

Current deep beam theory based design formulae are conservative for pile caps, and although the strut-and-tie method in UK standards BS 8110 gives a better prediction, it fails to do so for caps with large transverse pile spacing. The FEA has shown that transverse reinforcement plays an important role and the width of longitudinal reinforcement participating in the yielding tie can be larger than three times the pile diameter centred on each pile. A new strut-and-tie method is proposed, in which longitudinal reinforcement across 90% of the cap width is included in the ties, and the span of the longitudinal ties is slightly reduced to account for the pile diameter and width of the wall loading. This method improves the prediction of capacity especially for caps with large transverse pile spacing, provided that the longitudinal pile spacing is not excessively short and the cap fails in a ductile manner with yielding of the main longitudinal reinforcement.

Notation

a_v: Shear span

A : Shear enhancement application factor b_{enh}/b (evaluated to BS 8110 rules)

A_s: Total area of main reinforcement in cap longitudinal direction

b: Pile cap overall width

b_{enh}: Transverse width of cap on which shear enhancement applied

C : Compressive force in inclined strut in strut-and-tie model

d : Effective depth to main longitudinal reinforcement

d_p : Height of pile in experimental test and numerical model

f_{cu} : Concrete cube compressive strength

f_{ck}: Concrete cylinder compressive strength

f_t: Concrete tensile strength

f_y: Reinforcement yield strength

F : Load capacity of pile cap calculated from revised strut-and-tie method

h : Overall depth of pile cap

h_c: Width of wall loading

h_p: Pile diameter

L : Overall length of pile cap

l_x : Longitudinal pile spacing

l_y : Transverse pile spacing

v : Average shear stress on a vertical cross-section through a pile cap

V : Shear capacity of pile cap

z : Inner lever arm

α, γ : Space angles in strut-and-tie model

Bloodworth Cao & Xu

$\beta_{BS8110b}$:   Ratio of experimental failure load to BS 8110 bending theory based prediction

$\beta_{BS8110S}$:   Ratio of experimental failure load to BS 8110 strut-and-tie method prediction

β_{nSTM}:   Ratio of experimental failure load to revised strut-and-tie method prediction

γ_m: Partial factor on material strength in British Standards

ε^{cr}:   Crack strain

ε_{ult}^{cr}:   Ultimate crack strain

μ: Ratio of transverse pile spacing to pile diameter ($= l_y/h_p$)

σ_{sx}:   Reinforcement stress in longitudinal (x) direction

σ_{sy}:   Reinforcement stress in transverse (y) direction

σ_v: von Mises stress

References

AASHTO (2007). *LRFT Bridge Design Specifications*, 4th Ed. in SI units, American Association of State and Highway Transportation Officials, Washington, D.C., USA.

ACI (2005). *Building Code Requirements for Structural Concrete* (ACI 318-05) and *Commentary to the Building Code Requirements* (ACI 318R-05), American Concrete Institute, Farmington Hills, Michigan, USA.

Adebar, P. and Zhou, L. (1996). "Design of Deep Pile Caps by Strut-and-Tie Models." *ACI Structural Journal* 93(4), 437-448.

Bazant, Z. P., and Oh B.H. (1983). "Crack Band Theory for Fracture of Concrete." *Materials et Constructions*, 16, 155-177.

Bloodworth, A. G., Jackson, P. A., and Lee, M. M. K. (2003). "The Strength of Reinforced Concrete Pile Caps." *ICE Proceedings Structures and Buildings* 156(4), 347-358.

BSI (1997). *BS 8110: Structural use of concrete: Part 1: Code of practice for design and construction.* British Standards Institution, Milton Keynes.

BSI (1990). *BS 5400: Steel, concrete and composite bridges: Part 4: Code of practice for design of concrete bridges.* British Standards Institution, Milton Keynes.

BSI (2004). *BS EN 1992-1-1: Design of concrete structures — Part 1-1: General rules and rules for buildings.* British Standards Institution, Milton Keynes.

BSI (2005). *BS EN 1992-2: Eurocode 2 — Design of concrete structures — Part 2: Concrete bridges — Design and detailing rules.* British Standards Institution, Milton Keynes.

Cao, J. (2009). "The shear behaviour of the reinforced concrete four-pile caps." PhD Thesis, University of Southampton, UK.

Cao, J. and Bloodworth, A.G. (2011). "Shear behaviour of reinforced concrete pile caps under full-width wall loading." *Accepted for publication in Proceedings of the Institution of Civil Engineers, Structures and Buildings.*

Cao, J., Bloodworth, A.G. and Xu, M. (2007). "Observations of truss action in reinforced concrete pile caps." *Proc. 3rd Int. Conf. on Structural Engineering, Mechanics and Computation, Cape Town, South Africa.*

Clarke, J. L. (1973). *Behaviour and Design of Pile Caps with Four Piles*, Cement and Concrete Association, Technical Report, 124-136.

CSA (1994). *Canadian Standard for the Design of Concrete Structures* (A23.3-94), Canadian Standards Association, Mississauga, Ontario, Canada.

DIANA (2002). *DIANA finite element analysis user's manual release 8.1.* TNO DIANA BV, Delft, The Netherlands.

DIANA (2005). *Standard DIANA course tutorials and exercises*. TNO DIANA BV, Delft, The Netherlands.

Keown, P. G. (2000). "Investigation of the shear characteristics of reinforced concrete continuous beams." PhD Thesis, Queen's University, Belfast, UK.

Park, J., Kuchma, D. and Souza, R. (2008). "Strength predictions of pile caps by a strut-and-tie model approach." *Canadian Journal of Civil Engineering*, 35(12), 1399-1413.

Regan, P. E. (1971). *Shear in Reinforced Concrete – an Analytical Study*. Construction Industry Research and Information Association, Imperial College, London.

Table 1 Batch 4 experimental sample details

Pile cap Ref.	Cap length L (mm)	Cap width b (mm)	Longitudinal pile spacing l_x (mm)	Transverse pile spacing l_y (mm)	Ratio transverse pile spacing to pile diameter $\mu = {l_y}/{h_p}$	Ratio of shear span to effective depth $\dfrac{a_v}{d}$	Shear enhancement application factor A (BS8110)	Reinforcement diameter (mm) / ratio $\dfrac{100 A_s}{bd}$ (%)	Concrete cylinder strength f_{ck}/ cube strength f_{cu} (N/mm^2)
B4A1	1100	500	800	300	2.31	1.56	1	12 /1.137%	16.2/20.3
B4A2	950	500	650	300	2.31	1.18	1	12 /1.137%	17.4/21.8
B4A3	850	500	550	300	2.31	0.93	1	12 /1.137%	19.4/24.3
B4A4	800	500	500	300	2.31	0.81	1	12 /1.137%	19.5/24.4
B4A5	700	500	400	300	2.31	0.56	1	12 /1.137%	18.4/23.0
B4B1	950	500	650	300	2.31	1.18	1	10 /0.786%	15.6/19.5
B4B2	950	650	650	450	3.46	1.18	0.908	10 /0.786%	20.5/25.6

| B4B3 | 950 | 750 | 650 | 550 | 4.23 | 1.18 | 0.787 | 10 /0.786% | 19.8/24.7 |
| B4B4 | 950 | 900 | 650 | 700 | 5.38 | 1.18 | 0.67 | 10 /0.786% | 16.8/21.0 |

Table 2 Comparison of the failure loads between experiments and FEA

Pile cap Ref.	Failure load in experiments V (kN)	Prediction by FEA (kN)	Ratio failure load in FEA to experiments
B4A1	592	632	1.07
B4A2	548	820	1.50
B4A3	919	1008	1.10
B4A4	1052	1064	1.01
B4A5	1244	1244	1.00
B4B1	622	605	0.97
B4B2	713	812	1.14
B4B3	769	924	1.20
B4B4	1048	1040	0.99
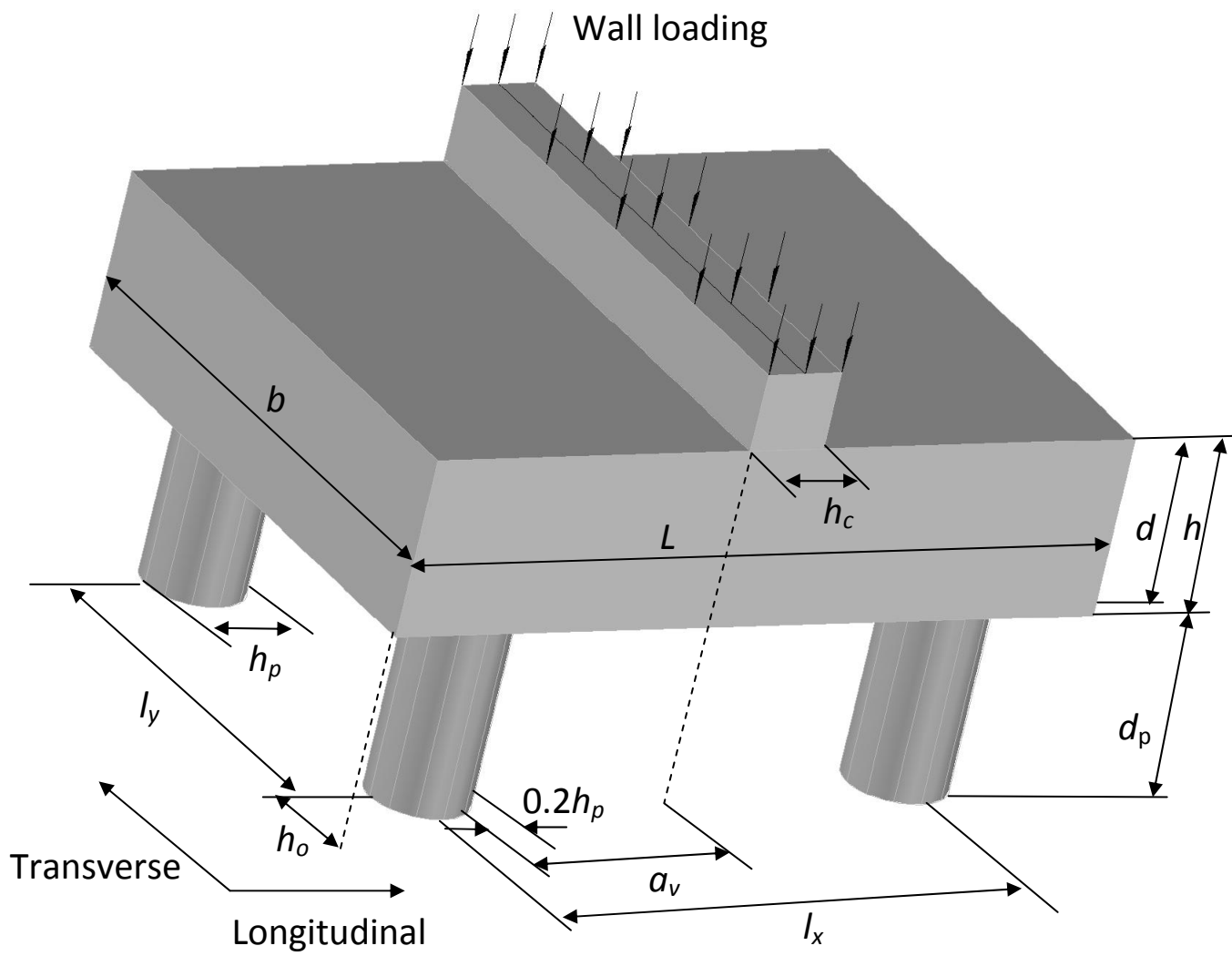
Figure 1 RC four-pile cap under a full-width wall loading
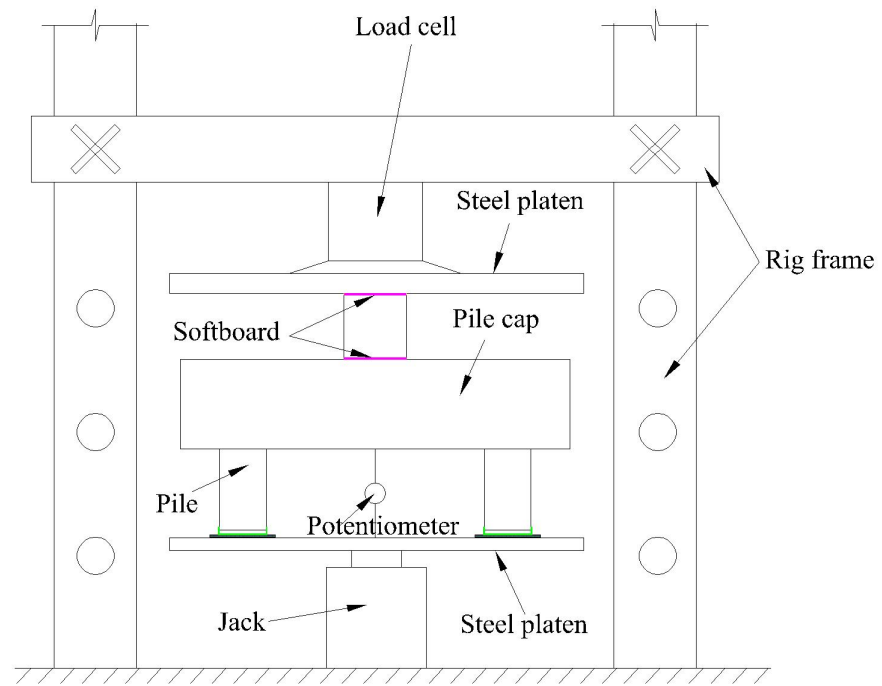
Figure 2 Experimental arrangement schematic
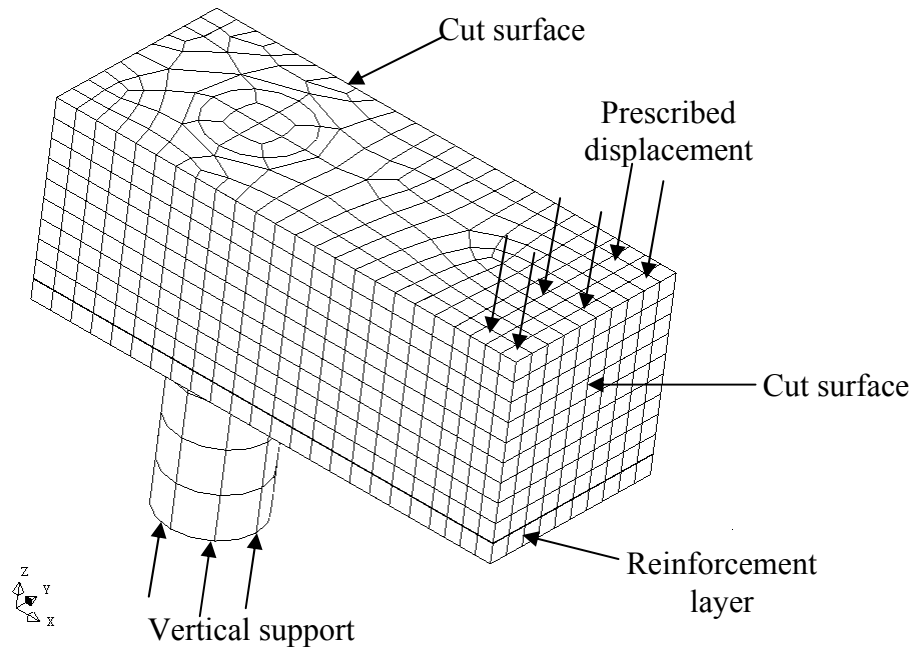
Figure 3 Geometry and mesh division of FEA model of a quarter pile cap
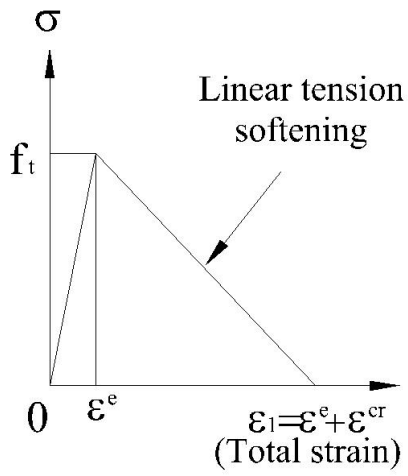
Figure 4 Constitutive relation of concrete in tension
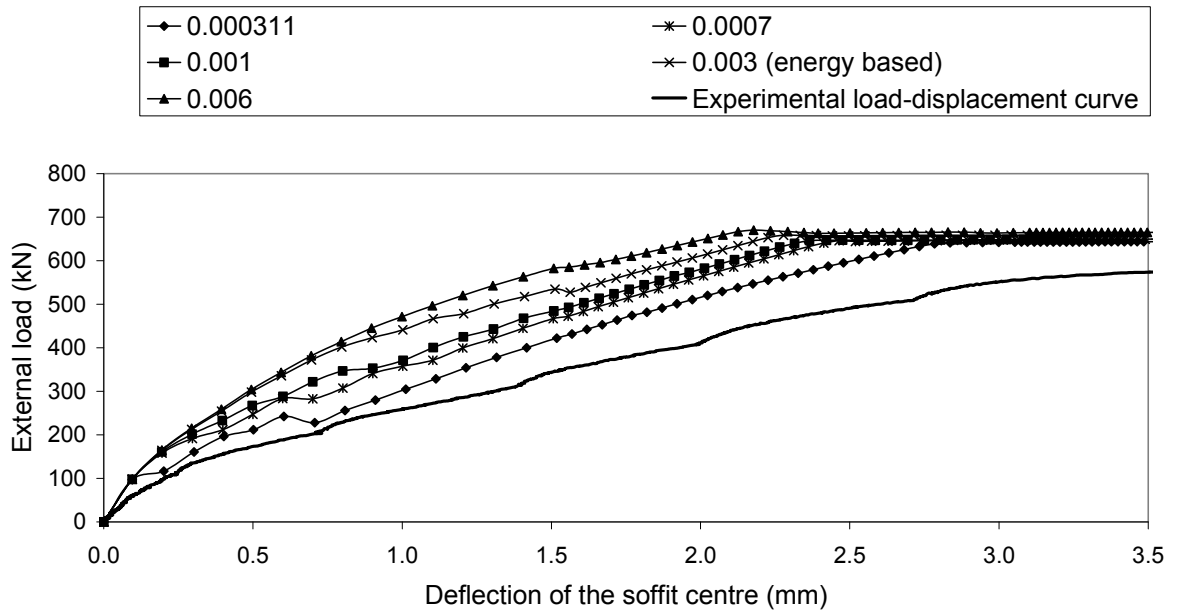
Figure 5 Sensitivity of load-displacement curve to values of ultimate crack strain ε_{ult}^{cr} for cap B4A1
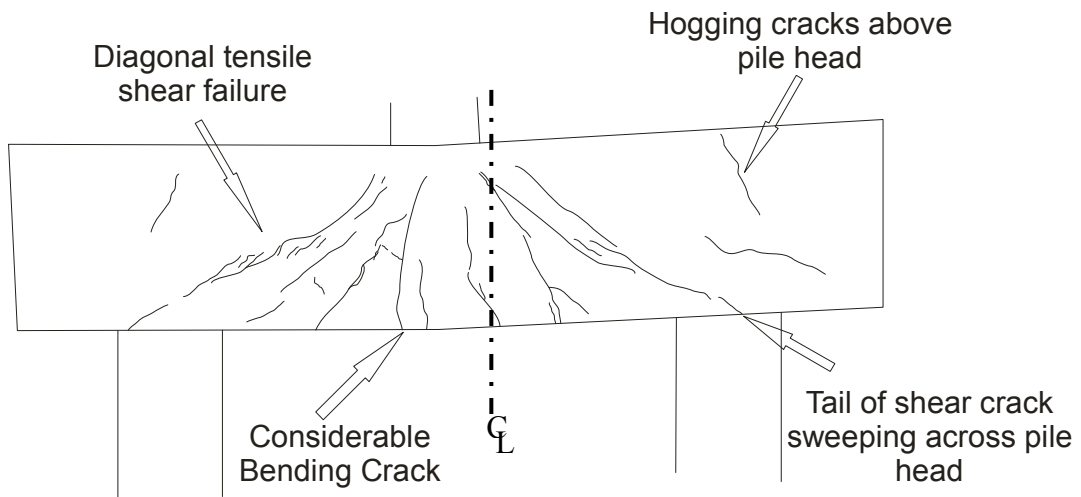
(a) Crack pattern on front surface observed in experiment

Crack strain ε^{cr}
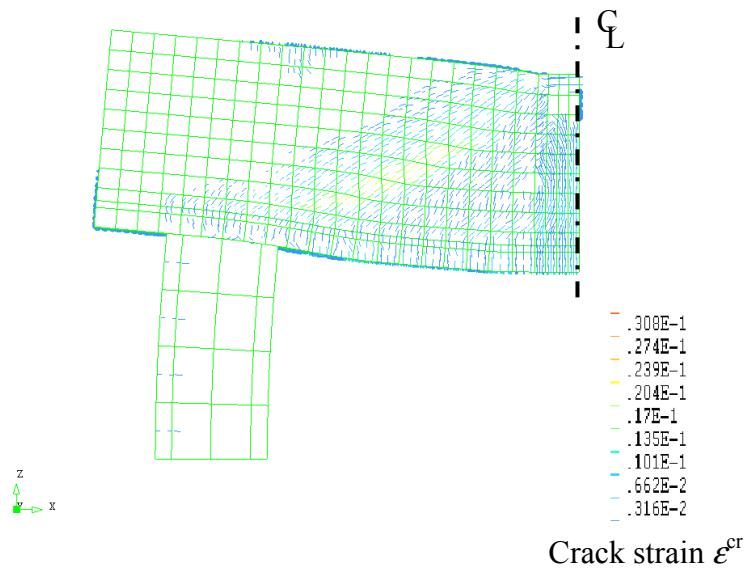
(b) Crack distribution on front surface in FEA

Figure 6 Comparison of crack patterns from experiment and FEA with basic
parameters at failure for cap B4A1 ($a_v/d = 1.56$)
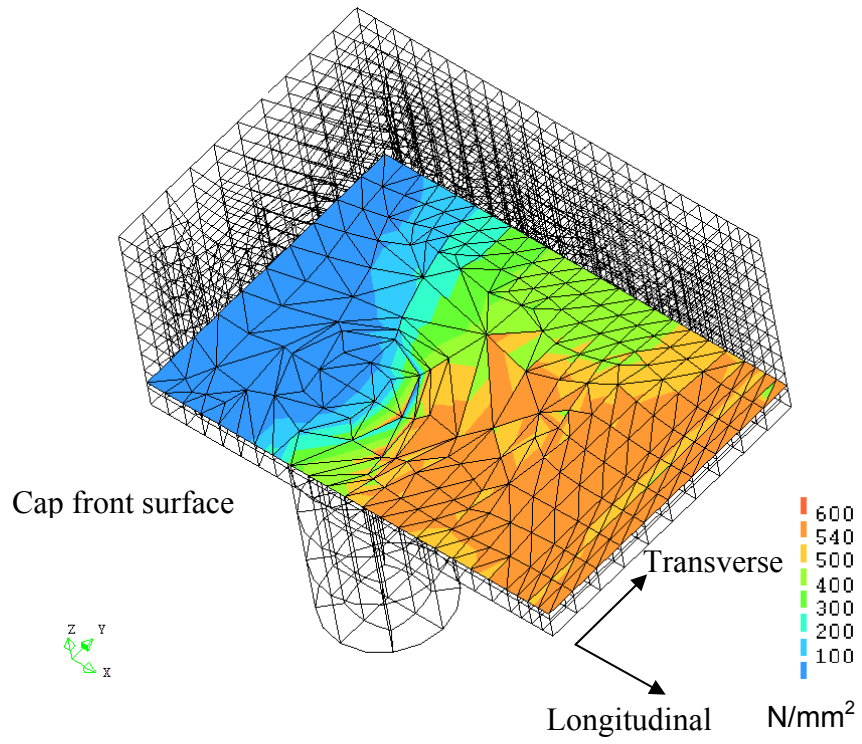
Figure 7 Longitudinal reinforcement stress σ_{sx} at failure for cap B4B2
($\mu = 3.4$, $a_v/d = 1.18$)
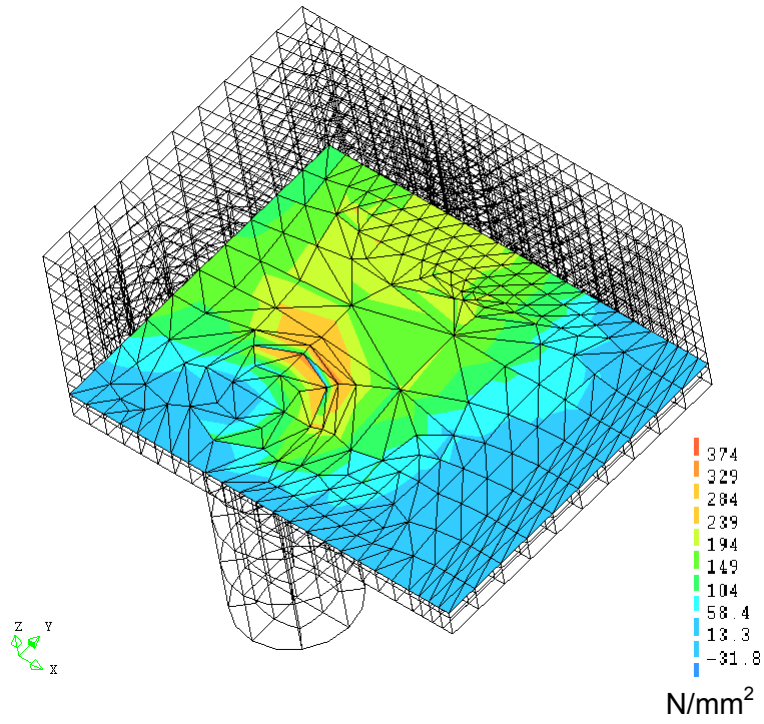
Figure 8 Transverse reinforcement stress σ_{sy} at failure for cap B4B3

($\mu = 4.2$, $a_v/d = 1.18$)

Equivalent compressive strut
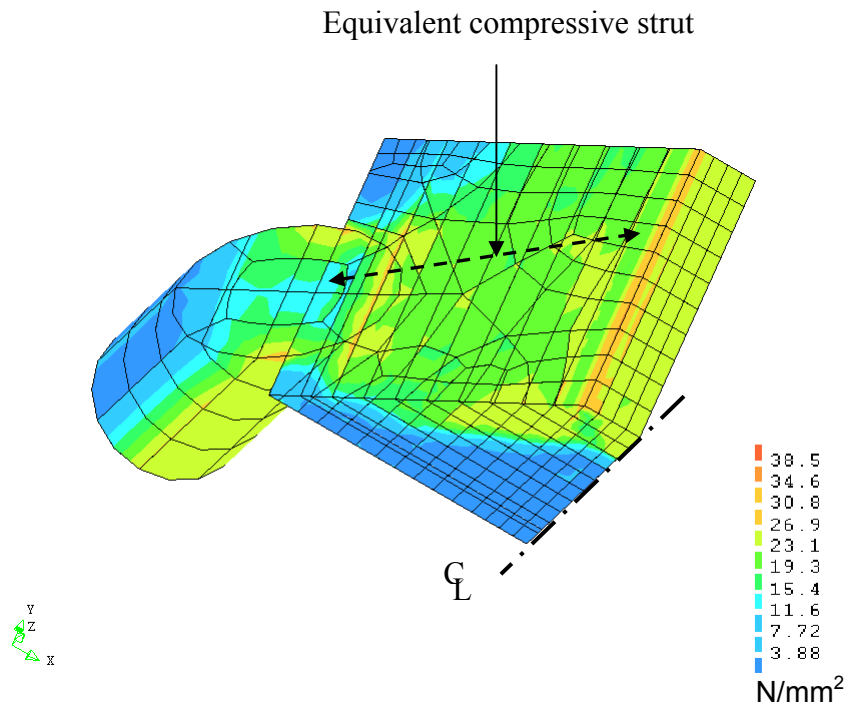
(a) contour of von Mises stress σ_v
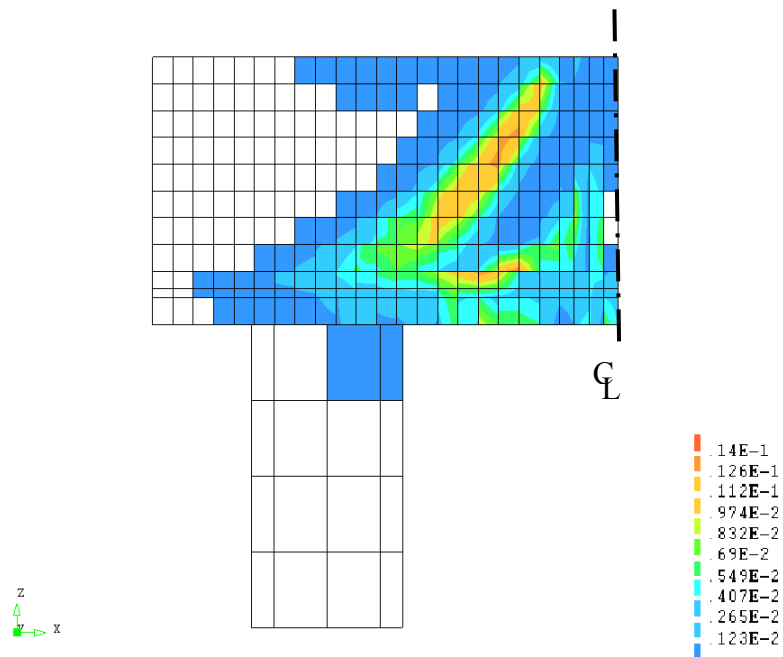
(b) contour of cracking strain ε^{cr} on front surface

Figure 9 Strut-and-tie behaviour at the onset of yield for cap B4A4

$(\mu = 2.3, \ a_v/d = 0.81)$

Longitudinal pile spacing l_x (mm) ($\frac{a_v}{d}$)	Transverse pile spacing l_y (mm) (μ)										
	150 (1.15)	200 (1.54)	260 (2.00)	300 (2.31)	350 (2.69)	390 (3.00)	500 (3.84)	600 (4.62)	800 (6.15)	1000 (7.69)	1200 (9.23)
300 (0.31)											
350 (0.43)											
390 (0.53)											
500 (0.81)											
600 (1.06)											
800 (1.56)											
1000 (2.06)											
1200 (2.56)											

	Shear failure
	Bending failure

Figure 10 Occurrence of shear or bending failure as indicated by cracking on cap front surface for models in parametric study (All dimensions in mm)
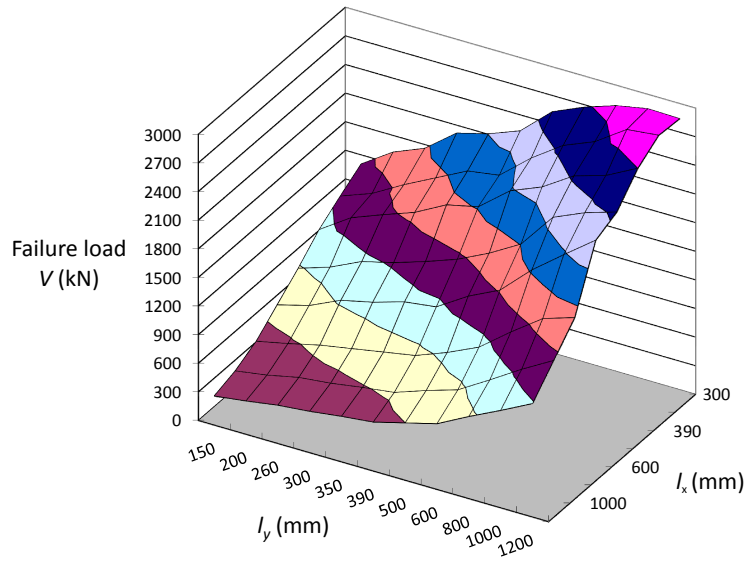
Figure 11 Variation of failure load V for models in parametric study against longitudinal pile spacing l_x and transverse pile spacing l_y
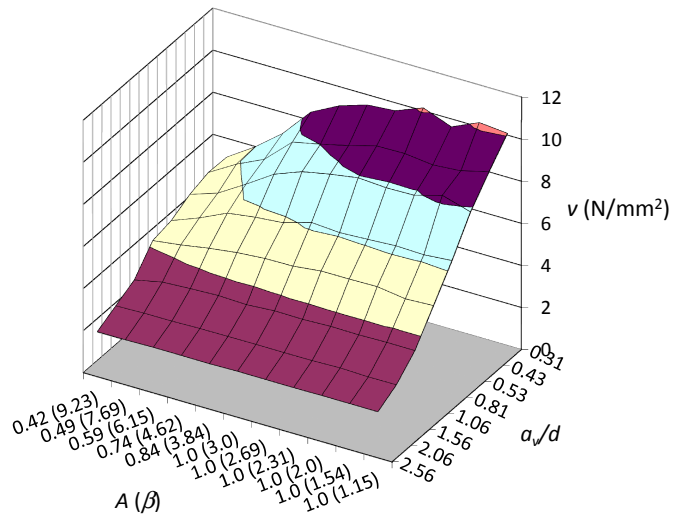
Figure 12 Variation of average shear stress *v* with *A* and a_v/d

for models in parametric study
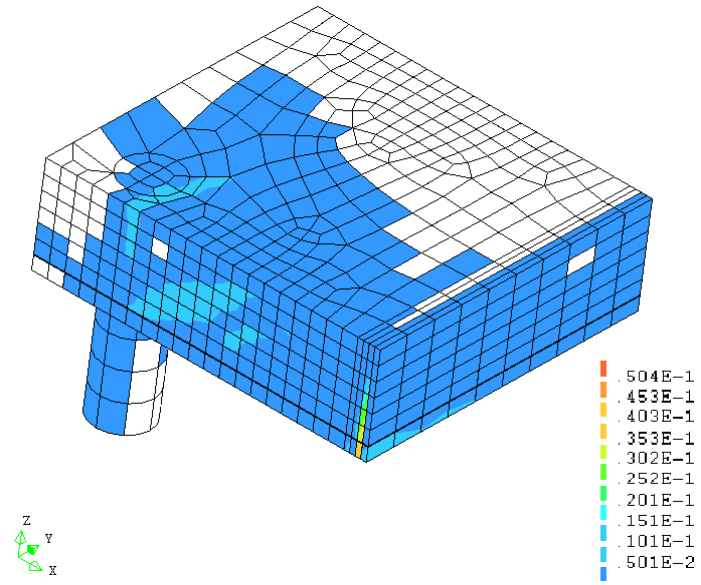
Figure 13 Bending failure shown by crack strain ε^{cr} on front surface of cap with

$\mu = 9.23$, $a_{v}/d = 2.56$
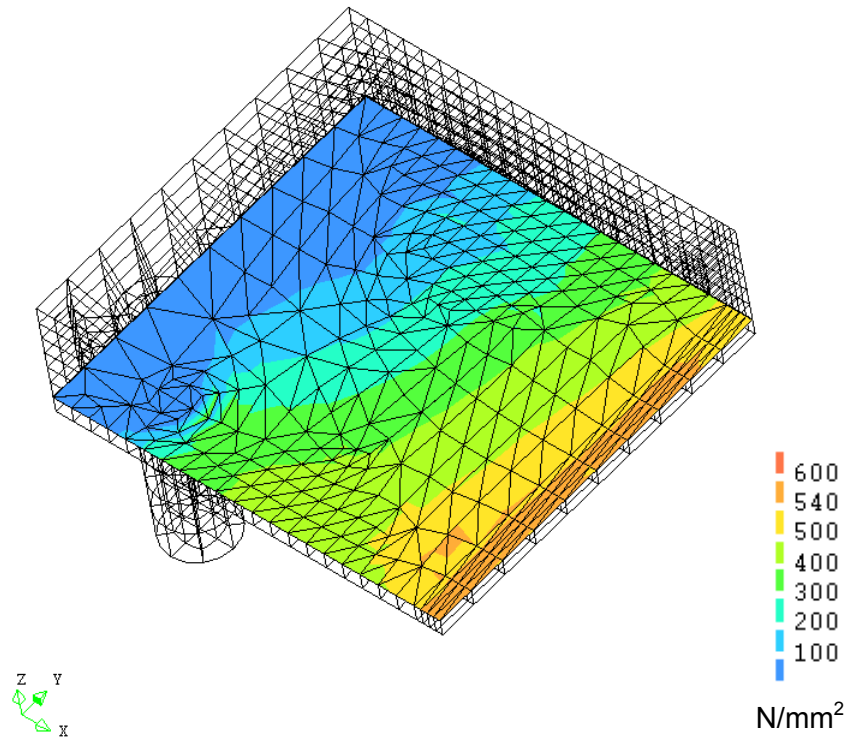
Figure 14 Longitudinal reinforcement stress σ_{sx} at failure for cap with $\mu = 9.23$, $a_v/d = 2.56$

Longitudinal pile spacing l_x (mm) ($\frac{a_v}{d}$)	Transverse pile spacing l_y (mm) (μ)				
	500 (3.84)	600 (4.62)	800 (6.15)	1000 (7.69)	1200 (9.23)
300 (0.31)					
350 (0.43)					
390 (0.53)					
500 (0.81)					
600 (1.06)					
800 (1.56)					
1000 (2.06)					

	Longitudinal reinforcement not yielded on whole cap width

Figure 15 Occurrence of yielding longitudinal reinforcement on the whole cap width

at midspan for models in parametric study (All dimensions in mm)
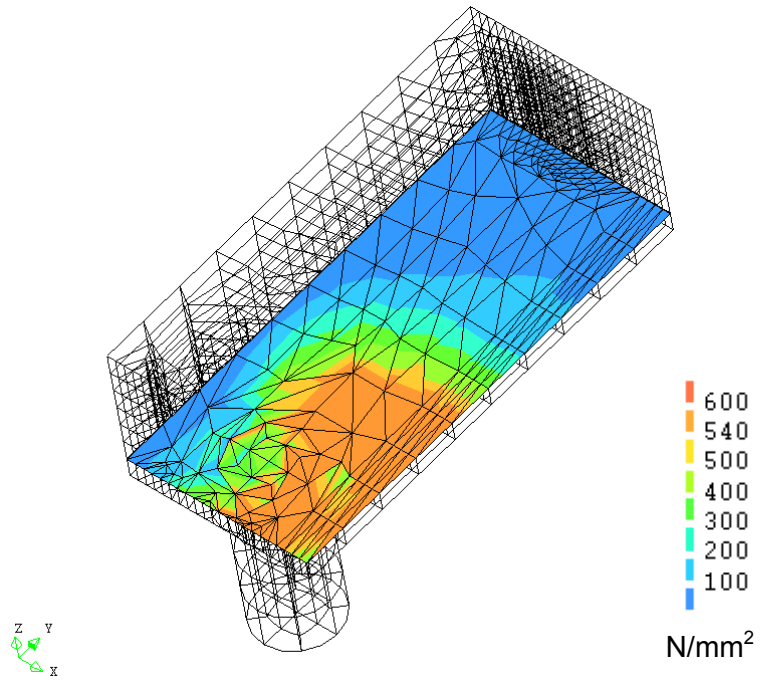
Figure 16 Longitudinal reinforcement stress σ_{sx} at failure for cap with $\mu = 9.23$, $a_v/d = 0.31$
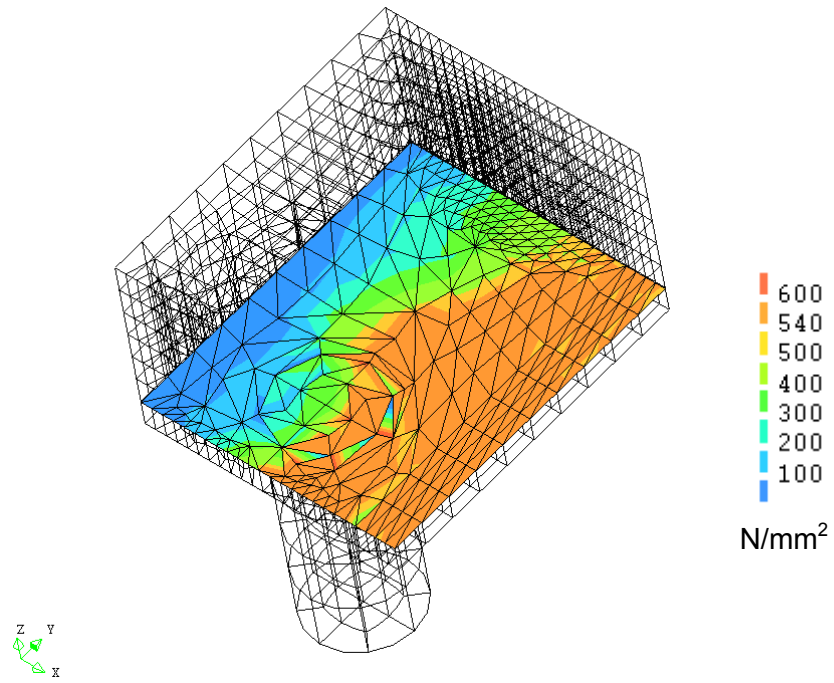
Figure 17 Longitudinal reinforcement stress σ_{sx} at failure for cap with $\mu = 4.62$, $a_v/d = 0.43$
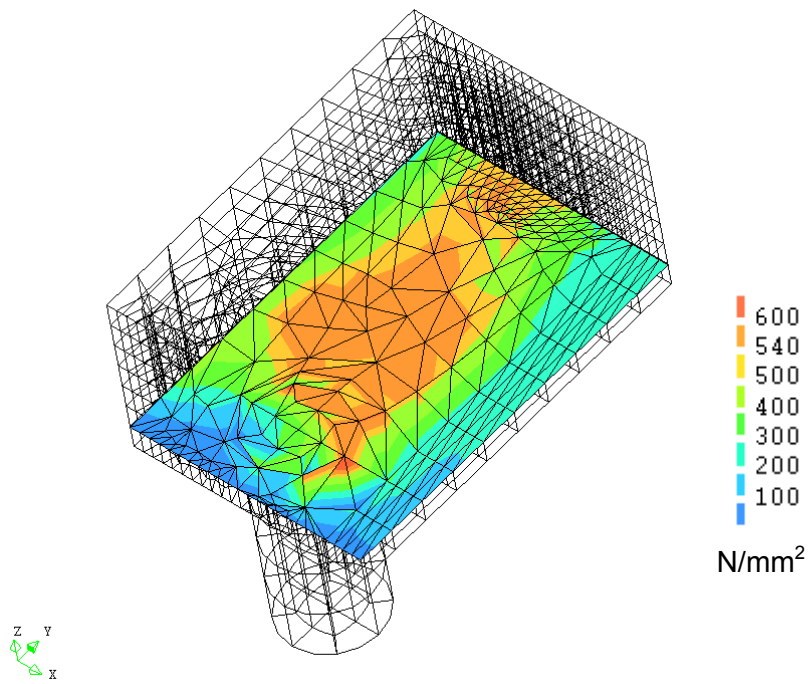
Figure 18 Transverse reinforcement stress σ_{sy} at failure for cap with
$\mu = 6.15$, $a_v/d = 0.43$
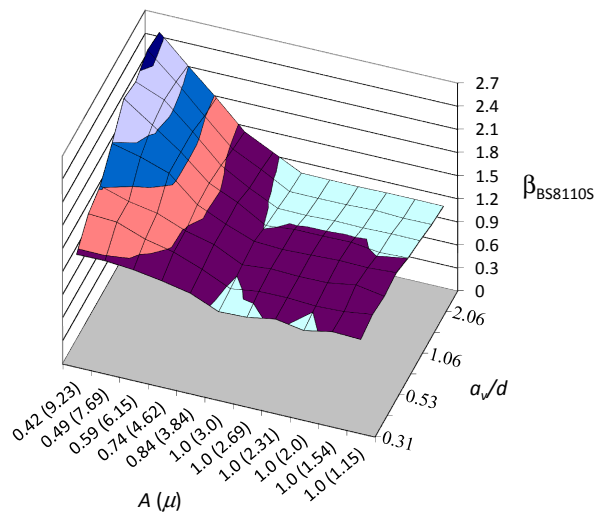
Figure 19 Variation of $\beta_{BS8110S}$ with A and a_v/d for 88 models in parametric study
$(\gamma_m = 1)$
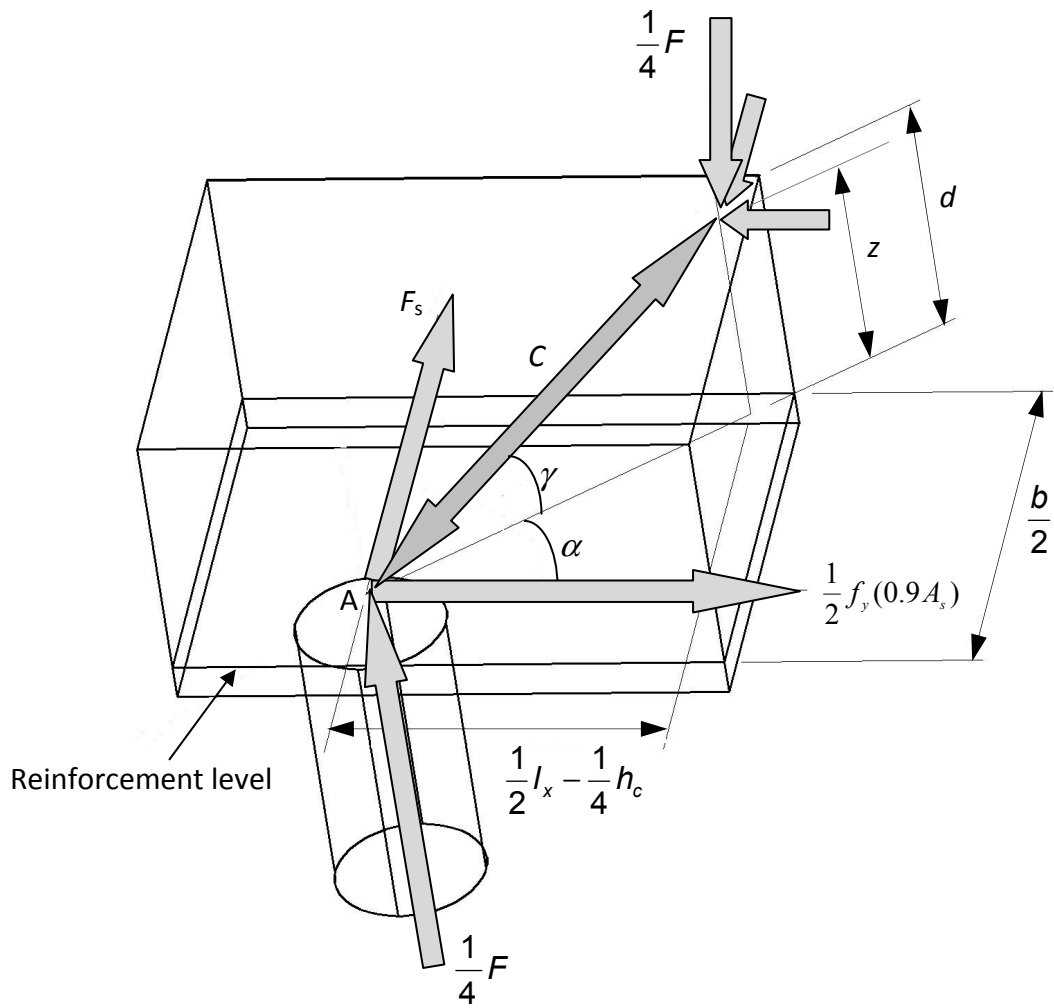
Figure 20 Proposed modified strut-and-tie model shown for a ¼ pile cap
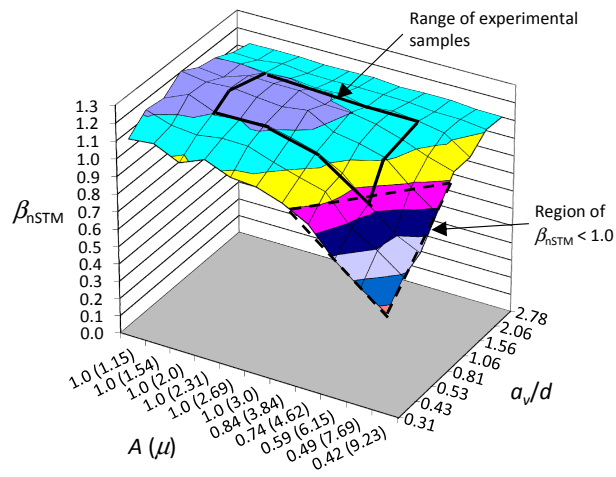
Figure 21 Variation of β_{nSTM} with A and a_v/d for 88 models in parametric study ($\gamma_m = 1$)